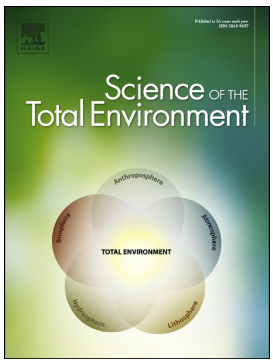

Spatial relationships between ecosystem services and socioecological drivers across a large-scale region: A case study in the Yellow River Basin

Yushuo Zhang, Xiao Lu, Boyu Liu, Dianting Wu, Guo Fu, Yuntai Zhao, Piling Sun

PII: S0048-9697(20)36009-5

DOI: https://doi.org/10.1016/j.scitotenv.2020.142480

Reference: STOTEN 142480

To appear in: *Science of the Total Environment*

Received date: 25 April 2020

Revised date: 15 September 2020

Accepted date: 16 September 2020

Please cite this article as: Y. Zhang, X. Lu, B. Liu, et al., Spatial relationships between ecosystem services and socioecological drivers across a large-scale region: A case study in the Yellow River Basin, *Science of the Total Environment* (2020), https://doi.org/10.1016/j.scitotenv.2020.142480

Spatial relationships between ecosystem services and socioecological drivers across a large-scale region: A case study in the Yellow River Basin

Yushuo Zhang[a]*, Xiao Lu[b,c]*, Boyu Liu[d], Dianting Wu[e], Guo Fu[f], Yuntai Zhao[g], Piling Sun[c]

a Faculty of Culture Tourism, Shanxi University of Finance and Economics, Taiyuan 030006, China

b School of Humanities and Law, Northeastern University, Shenyang 110169, China

c School of Geography and Tourism, Qufu Normal University, Rizhao 276826, China; sapphire816@163.com

d College of Mining Engineer, Taiyuan University of Technology, Taiyuan 030024, China; liuby10@mails.jlu.edu.cn

e Faculty of Geographical Science, Beijing Normal University, Beijing 100875, China; wudianting@bnu.edu.cn

f School of History, Culture and Tourism, Liaoning Normal University, Dalian 116081, China; 272622193@qq.com

g Chinese Land Surveying and Planning Institute, Beijing 100035, China; zhaoyuntai@163.com

* Correspondence: zhangys@sxufe.edu.cn (Y Zhang); lvxiao@mail.neu.edu.cn (X Lu); Tel.: +86-152-3512-7056 (Y Zhang)

Acknowledgements

This research was funded by the National Natural Science Foundation of China (41771128, 41671176),

Humanities and Social Science Fund of Ministry of Education of China(19YJA890006), and LiaoNing Revitalization Talents Program (XLYC1807060). Thanks, are extended to Editage (www.editage.cn) and Elsevier Language Editing Services for the help of English language editing.

Author Contributions

Y Zhang and X Lu designed the study, collected the database, and performed the research. Y Zhang

analyzed data, and wrote the paper. B Liu participated in data processing and model calculation. The

remaining authors contributed to discuss the results and revise the manuscript. All authors have read and approved this manuscript.

Spatial relationships between ecosystem services and socioecological drivers across a large-scale region: A case study in the Yellow River Basin

Abstract: Understanding the relationships between ecosystem services (ES) and their underlying socioecological drivers is essential for forming the efficient management decisions of ecosystems. We use a large watershed area as a case-study to analyze trade-offs/synergies and bundles of ESs and identify the associated socioecological variables (SEVs). This study assessed the supply of 7 ES indicators, namely, three provisioning services (crop production, livestock production, and industrial production), three regulating services (water conservation, soil conservation, and carbon sequestration), and one cultural service (recreation), across 65 municipalities in the Yellow River Basin (YRB) in China. We analyzed the paired trade-offs/synergies using Spearman's coefficient and identified the ES bundles (ESBs) by applying principal component analysis and K-means clustering. Subsequently, we detected the SEVs that affect the ES supply using the geo-detector model and characterized the associations between ESBs and socioecological clusters according to the spatial overlap. The results demonstrated that the synergies between ESs substantially exceeded the trade-offs, among which the strongest synergies were between the crop production and the livestock production, and both responded strongly to the cropland and the population density. Trade-offs were identified between provisioning services and soil conservation. Municipalities were grouped into three ESBs in the YRB. The ESB, which was dominated by provisioning ESs, was associated with areas where cropland, precipitation and

socioeconomic conditions were all important, and the regulation of ESB was linked to regions with distinct ecological characteristics. We also identified an ESB that was dominated by carbon sequestration, as determined by extensive grassland and bare land. The land use/land cover strongly affected the characteristics of the ESBs. The findings can be used by land managers to identify areas in which ESs are dominant, to determine the associations of these compositions of the ESs with SEVs, and to support the formulation of optimal ES management in large-scale basins.

Keywords: ecosystem service; spatial relationships; socioecological driver; Yellow River Basin

1. Introduction

Ecosystem services (ESs) are defined as the benefits that humans directly or indirectly receive from ecosystems (Costanza et al., 1997). The Millennium Ecosystem Assessment (MA, 2005) developed a classification framework for ecosystem assessments around the world. This framework categorized available ES indicators into provisioning, regulating, cultural and supporting services based on the linkage between ESs and human well-being, among which supporting services are the basis for the maintenance and supply of the other three services. There are important dynamically complex relationships among the ESs that can lead to simultaneous positive and negative changes in the provision of ESs (Bennett et al., 2009). A trade-off occurs when the provision of an ES is reduced due to the increased use of another ES (Rodríguez et al., 2006; Raudsepp-Hearne et al., 2010), while synergy arises when multiple ESs are

enhanced simultaneously (Tomscha and Gergel, 2016), which is a win-win scenario (Qiu and Turner, 2013). The ES bundle is the repetitive occurrence of trade-offs and synergies of ES across space and time (Raudsepp-Heard et al., 2010; Cord et al., 2017), which reflects the ES relationships by focusing on inherent bundles of ESs rather than on individual ESs (Turner et al., 2014). Understanding these relationships is important for making efficient decisions regarding rational ecosystem-based management. Furthermore, the identification of the drivers and mechanisms that underlie the ES relationships is necessary for better understanding the possibility of forming these relationships (Bennett et al., 2009; Dade et al., 2018). Several studies are focused on the trade-offs and synergies of ESs that are driven by social and ecological variables across the region (Ndong et al., 2020). However, understanding of the relative importance of socioecological drivers to the ES supply and the relationships between ESs remains limited.

The methodology of the ES bundle enables the capture of inclusion and the geographical visualization of multiple ESs, simultaneously to generate geographical and statistical mappings of ES bundles that can indicate which services associated with each other based on where they were found repeatedly occurring together (Raudsepp-Heard et al., 2010). This approach has increasingly been applied to the spatial identification of the relationships between ESs and their drivers (e.g., Queiroz et al., 2015; Dittrch et al., 2017; Spake et al., 2017; Lyu et al., 2019) at, for example, the national, regional, and watershed scales. The driving variables can be determined by interpreting the spatial distribution of ES bundles with respect to known distributions of principal natural variation and human

activities within the study area. Nevertheless, distinct bundles are likely produced by different sets of socioecological drivers that are targeted towards bundles of services instead of individual services (Spake et al., 2017). This bundle approach can be used to identify the clusters of socioecological drivers that spatially overlap with ES bundles to detect the dominant driving variables of each ES bundle. Therefore, the bundle approach is regarded as efficient for predicting the spatial relationships between ESs and conveying information on consistent associations to decision-makers (Cruzat et al., 2015; Ndong et al., 2020).

Drivers are the variables that cause ES relationships to develop or change (Bennett et al., 2015). The land use/land cover (LULC) (e.g., vegetation cover or land use) has been identified most as the determinant of ES relationships (Dade et al., 2018). For example, Grimaldi et al. (2014) showed that the land-cover composition dynamics explained 45% of the ES metric variance. Spake et al. (2017) showed that crop-dominant bundles were associated with the agricultural land coverage and that forest service-dominant bundles were associated with high forest cover. In addition, biophysical and socioeconomic variables were also commonly regarded as important drivers of ES relationships (Dade et al., 2018; Ndong et al., 2020). Substantial effort is being focused on investigating the socioecological conditions that are behind the occurrence of ES bundles (Gonzalez-Ollauri and Mickovski, 2017). In large-scale regions such as basins and surrounding areas, most of the current studies focus on biophysical variables (e.g., climate variability, wind erosion, hydrological effects, and soil properties) and policy instruments such as vegetation restoration policy. Socioeconomic variables have received

less attention in large-scale basins (Feng et al., 2017; Rositano et al., 2018; Jiang et al., 2018), and the relative importance of socioecological drivers of ES relationships remains unclear. Socioeconomic variables also influenced the co-occurrence of trade-offs/synergies and ES bundles in a large-scale basin (Qiu and Turner, 2013; Queiroz et al., 2015; Meacham et al., 2016). Therefore, research is necessary for exploring the socioecological drivers of spatial relationships between ESs in a large-scale basin.

The Yellow River Basin (YRB) is a large-scale basin across northern China, which includes the Qinghai-Tibet Plateau, the Loess Plateau and the North China plain, from west to east, with substantial differences in natural and socioeconomic conditions. It is an important source of freshwater in northern China. Under the pressures of harsh ecological conditions and economic growth (Su et al., 2012), the natural and seminatural ecosystems of the YRB have become increasingly fragile. For instance, water depletion and wetland shrinkage in the upper reaches of the YRB have threatened the supply of freshwater resources of the YRB (Zhang et al., 2012; Jiang et al., 2015). Severe soil erosion that is caused by a thick mantle of loess, dry climate, and complex topography is a direct threat to the conservation of water and soil in the middle and lower reaches of the YRB (Bing et al., 2011). Although ecological restoration programs have promoted the restoration of forest and grassland, they have not improved the anti-erosion performance of the soil in the middle reaches of the YRB (Jiang et al., 2016). The fragility of the ecosystems has constrained the supply of ESs and the social and economic development in the YRB (Li et al., 2016; Chi et al., 2018; Wang et al., 2019).

Current studies on the ES relationships of the YRB have focused mainly on a set of soil and water conservation services in ecologically fragile areas at local and regional scales, such as the Loess Plateau region (Jiang et al., 2016; Wang et al., 2019), the Three-river headwater region (Jiang et al., 2016; Han et al., 2017), desert and semidesert regions (Li et al., 2017), and the Yellow River Delta region (Chi et al., 2018; Ma et al., 2019). For example, a significant trade-off between water provision and soil retention was identified in the Loess Plateau in the upper and middle reaches of the YRB (Jiang et al., 2016). However, a socioecological perspective from which to consider the systematic characteristics of relationships between ESs and the socioecological drivers in the YRB is lacking (Fu et al., 2015; Lyu et al., 2019). Such a perspective will increase our understanding of ES relationships and improve the ability to sustainably manage ESs in a large-scale basin. Therefore, multiple ESs and their relationships must be seriously considered instead of merely focusing on soil and water conservation for the priority of ecological governance in such a large-scale basin (Qiu and Turner, 2013; Queiroz et al., 2015).

Focusing on the YRB as a case study, we aim to analyze trade-offs/synergies and bundles of ESs and identify the associated socioecological variables. The objectives of this study are to (i) quantify and map the spatial distribution of ESs; (ii) analyze the pairwise correlations between ESs and characterize the ES bundles; (iii) identify the socioecological drivers; and (iv) assess the associations between ES bundles and socioecological clusters. The results are expected to provide useful information for equilibrating economic development and ecological restoration in large-scale basins.

2. Materials and Methods

In this study, the ES indicators are assessed in the YRB, and the relationships between ESs are examined utilizing correlation analysis and the ES-bundle approach. Then, the social-ecological drivers are identified for the correlation of ESs and the occurrence of ES bundles to mitigate trade-offs and enhance synergies among ESs. Municipal boundaries are used to distinguish the spatial units because they represent the most efficient administrative boundaries for socioecological governance. In addition, these boundaries may be able to represent the social processes that shape the production and consumption of ESs (Raudsepp-Heard et al., 2010) in the YRB. Importantly, they define the optimum spatial unit at which social and economic census data are available (Dittrich et al., 2017).

2.1. Study area

The YRB is situated in the northern part of China (31°31'N~43°31'N, 89°19'E~119°39'E) and covers 1.82 million km^2, thereby accounting for 19% of the territory of the country (Fig. 1 a). It mainly covers eight provincial-level administrative regions, namely, Qinghai, Gansu, Ningxia, Inner Mongolia, Shaanxi, Shanxi, Henan, and Shandong (Fig. 1 b), which include 65 municipalities (provincial capitals, autonomous prefectures, and prefecture-level cities) (Fig. 1 e). The average size of the municipalities is 27,979 km^2, and they range in size from 1,656 km^2 (Wuhai, Inner Mongolia) to 253,015 km^2 (Haixi, Qinghai). According to the China Statistical Yearbook (2018), the population of the study area accounted for 14.7% of the population of China in 2017, and it contributed

14.5% of China's GDP. The Chinese government put forward the objectives of "ecological protection and high-quality development" for the YRB in 2019 (Xi, 2019). Hence, the YRB is regarded as an ecological restoration zone in China, and ecological protection has been implemented as the premise for economic growth since the policy announcement.

The study area belongs to the temperate region, with an annual average temperature of 1–8 °C in the west, 8–14 °C in the middle, and 12–14 °C in the east. The topography is highly complex, with altitudes from -65 to 6813 m above sea level (Fig. 1 c). It has a climate gradient from continental arid and semiarid in the west to maritime semihumid in the east, with an annual average rainfall of 466 mm (Fig. 1 d). The upper reaches of the YRB in the western parts, which belong to the Qinghai-Tibet Plateau (Fig. 1 c), are the main water-yielding areas and provide freshwater resources for agricultural, industrial, and ecological demands throughout the YRB. The main land cover types in this area are alpine meadows, deserts, and lakes (Fig. 1 f). In the upper and middle reaches, the Loess Plateau is one of the most severe soil erosion regions in the world (LÜ et al., 2012). The dominant land cover types include grassland, desert, forest, and cropland (Su and Fu, 2013) (Fig. 1 f). The lower reaches of the YRB belong to the plain areas, which are dominated by cropland and provide food production services (Wang et al., 2019). There are substantial gaps in the levels of socioeconomic development in the northwest-southeast orientation of the YRB, such as the population density (Treacy et al., 2018). Population growth, reclamation, deforestation, and urbanization accelerated water and land resource exploitation in highly populated municipalities (Fig. 1 e), thereby causing daunting challenges for ecosystem restoration in recent decades.

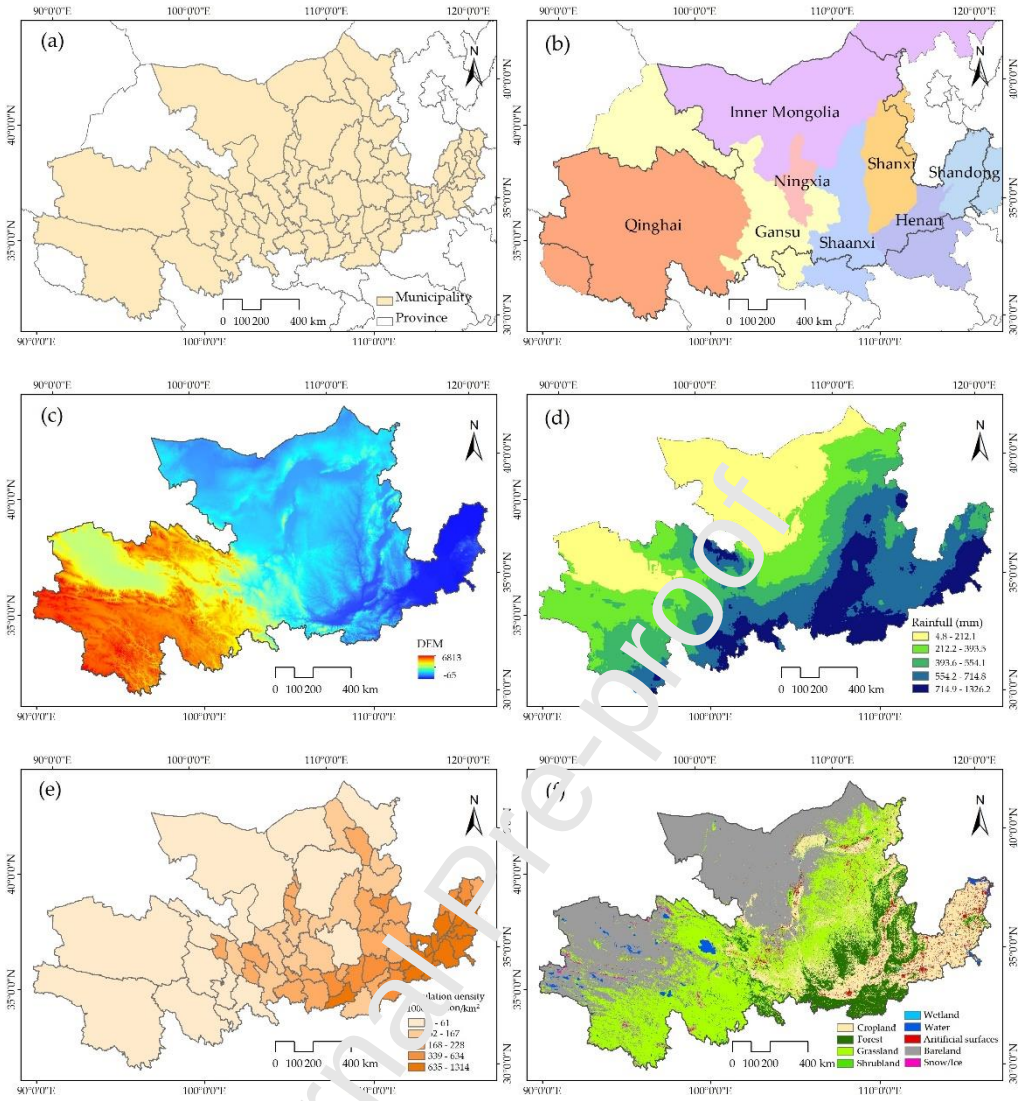

Fig. 1. Locations in the study area and general description of geographical information: (a) The location of the Yellow River Basin (YRB) on a map of China, (b) provincial administrative divisions of the YRB and neighboring areas, (c) a digital elevation model (DEM), (d) a spatial distribution of the yearly average rainfall, (e) the population density across 65 municipalities, and (f) land use and land cover types.

2.2. ES indicators

2.2.1. Data collection

The primary data that are necessary for the ES variables that are used to calculate the ES indicators are listed in Table 1. The land use/land cover data with 30 m resolution

(for water conservation, soil conservation and carbon sequestration) include nine land types: cropland, forest, grassland, shrubland, wetland, water, artificial surfaces, bare land, and snow/ice. Maps of the normalized difference vegetation index (NDVI) (for soil conservation and carbon sequestration) were constructed using the maximum composite value of MODIS NDVI data. A digital elevation model (DEM) (for soil conservation) was constructed from SRTM3 data with a spatial resolution of 90 m. The numeric-formatted meteorological data (for soil conservation and carbon sequestration) were derived from meteorological stations that were distributed throughout the YRB and the surrounding areas and interpolated to obtain raster-formatted data with a resolution of 1 km × 1 km to cover the whole study area using the kriging method in ArcGIS 10.0. Soil data (for soil conservation) were derived from the Harmonized World Soil Database (HWSD), and four indices were extracted: "Topsoil Sand Fraction (SAND, % wt)", "Topsoil Silt Fraction (SILT, % wt)", "Topsoil Clay Fraction (CLAY, % wt)" and "Topsoil Organic Carbon (OC, % weight)". All these primary data were integrated into a spatial resolution of 1 km × 1 km.

The administrative map, with the municipality as the spatial unit, was provided by the National Geomatics Center of China (NGCC) websites. Statistical data of crop yield and meat production (for crop production and livestock production, respectively) were derived from the Bulletin on National Economic and Social Development. The gross industrial output value (for industrial production) was derived from the statistical yearbooks for each municipality (e.g., Lanzhou Statistical Yearbook in 2018). The number of tourists (for recreation) was obtained from the China City Statistical Yearbook. These statistical data were expressed as spatial data in municipal units. All the spatial data were ultimately

unified to form the spatial reference (the WGS84 coordinate system and Albers equal-area conic projection).

Table 1

Summary of the ES variables for the assessment of ES indicators and their data types, time, spatial resolutions, and data sources.

ES variable	Data type	Time	Spatial resolution	Data source
Land use/land cover	Raster	2017	30 m	Data Center for Resources and Environmental Sciences of the Chinese Academy of Sciences: Resource and Environment Data Cloud Platform (http://www.resdc.cn/data.aspx?DATAID=99)
NDVI	Raster	2017	250 m	National Aeronautics and Space Administration and United States Geological Survey (http://e4ftl01.cr.usgs.gov/MOLT/MOD13Q1.006/)
DEM	Raster	2003	90 m	National Aeronautics and Space Administration and National Imagery and Mapping Agency (http://e0mss21u.ecs.nasa.gov/srtm/)
Precipitation and temperature	Numeric	1956-2017	Sites	Meteorological Data Center of China Meteorological Administration (http://data.cma.cn/)
Soil database	Raster	2009	30 arc-second	Harmonized World Soil Database v1.1 (http://www.fao.org/soils-portal/soil-survey/soil-maps-and-databases/harmonied-world-soil-datebse-v11/en/)
Administrative map	Vector	2017	municipality	National Geomatics Center of China

				(http://ngcc.sbsm.gov.cn/ngcc/)
Crop yield and meat production	Numeric	2017	municipality	Bulletin on National Economic and Social Development (2018)
Gross industrial output value	Numeric	2017	municipality	Statistical yearbooks of each municipality (2018)
Number of tourists	Numeric	2017	municipality	China City Statistical Yearbook (2018)

2.2.2. Selection of ES indicators

The selection of suitable ES indicators is a key challenge when assessing ESs (Wong et al., 2015). In this study, the criteria for the selection of ES indicators were as follows: (i) selection of those in the classification of ES by MA category (MA, 2005) to ensure comparability with other studies in this region because the MA classification system is a heuristic tool, (ii) selection of the ES indicators that were ecologically, socially and economically relevant to the YRB according to previous studies (Wong et al., 2015) and (iii) selection of the ES indicators for which the primary data that were required for the assessment were available (Bai et al., 2020). Based on these criteria, three ES categories and seven ES indicators were selected: provisioning services (crop production, livestock production, and industrial production), regulating services (water conservation, soil conservation, and carbon sequestration), and cultural services (recreation).

In this study, we explain the rationale for the selection of industrial production. Industrial production is important to economic growth and human well-being in the YRB because it partially substitutes ESs that are provided by natural ecosystems (Brauman et al., 2007) and, consequently, improves the supplies of other ESs indirectly. The economic

value of the industrial sectors is a direct benefit that human societies retrieve from the broad ecosystem (Yang et al., 2015).

2.2.3. Quantification of ESs

2.2.3.1. Provisioning services

Crop production (crop yield per square kilometer, ton/km^2): The processes that were used to assess the ES indicators in the study are listed in Table 2. The crop yield per square kilometer has been used as a proxy to quantify crop production (Yang et al., 2015). The amount of products from each crop yield (ton) in each municipality was obtained from the public datasets of statistical yearbooks (Table 1). It was estimated for the five major crop types: rice, wheat, corn, beans, and potatoes. The crop production was measured by dividing the crop yield of each municipality by its administrative boundary to calculate the per-unit provision service and was input into the attribute table of a vectorized municipality image for spatialization. Livestock production (production of pork, beef and mutton per square kilometer, ton/km^2): The amount of production of pork, beef and mutton (ton) per municipality was obtained from the public statistical yearbooks (Table 1). The category of meat products in the datasets provides the production of pigs, cattle, and sheep. Like the calculation method for the crop production (Table 2), the production of pork, beef and mutton was divided by the area of the municipality and was used to estimate the provision of livestock production. Industrial production (gross industrial output value per square kilometer, million yuan/km^2): Following a case study of the Yangtze River Delta in China (Yang et al., 2015), the gross industrial output value was selected as a proxy for the industrial production to represent the provision of industrial production of each

municipality (Table 2). The gross industrial output value (million yuan) was derived from the public city statistical yearbooks (Table 1).

2.2.3.2. Regulating services

Water conservation (water storage of forest per square kilometer, m^3/km^2): Water conservation was reflected mainly in the conservation of water by vegetation via the interception of precipitation, enhancement of soil infiltration, and inhibition of evapotranspiration (Bai et al., 2011). A major impact of land use on water conservation is the interception of surface water by vegetation. Based on the quantity of retained water, the method of water storage of forest ecosystems was used as the proxy for the water conservation of the YRB (Table 2), in accordance with Li (1999):

$$WC = \sum_{i=1}^{n} A_i \times P_i \times K_i \times R_i \qquad (1)$$

where *WC* refers to the amount of water conservation (m^3); *n* is the number of forest types in the YRB; A_i refers to forest area (km^2), which is derived from the land use/land cover data with 30 m resolution (Table 1); P_i is the annual average rainfall (mm) in the YRB, which is derived from meteorological site data and interpolated to form raster-formatted spatial data with a resolution of 1 km x1 km using the kriging method; K_i is the proportion of run-off of the total rainfall, which is 0.4 according to a previous study (Zhao et al., 2004); and R_i is the coefficient of the forest ecosystem type (forest, spinney or open woodland in the study area), which reduces the run-off compared with that of bare land and ranges from 0.21 to 0.39 across forest types. The water conservation values were calculated at 1 km x 1 km resolution, and this map was resampled for municipalities by the ArcGIS

module of zonal statistics to obtain an average water conservation value per municipality.

Soil conservation (soil conservation amount per hectare per annum, t/(hm²·a)): Soil conservation is the ability to reduce soil loss and land degradation, which represents the ecosystem function of preserving soil and water (Fu et al., 2015). It is critical for the wide arid and semiarid areas in the YRB (Su et al., 2012; Jiang et al., 2016). The universal soil loss equation (USLE) (Renard et al., 1991) was used to estimate the soil conservation as the difference between the potential and actual soil erosions. It has been validated by the example of Haihe River Basin (Ma, 1989), which showed that the soil erosion modulus calculated by this method is consistent with the measured values, and can meet the precision requirements of soil conservation evaluation in large basins. The equation is expressed as follows:

$$\Delta A = R \times K \times L \times S \times (1 - C \times P) \qquad (2)$$

where ΔA is the amount of soil that is conserved (t/(hm²·a)); R denotes the rainfall erosivity index (MJ·mm/(hm²·h·a)) (Wischmeier and Smith, 1978); K denotes the soil erodibility factor (t·hm²·h/(MJ·mm·hm²)) (Williams, 1990); L and S denote the slope length and slope steepness factors, respectively (unitless) (Mccool et al., 1989, Liu et al., 2000); C denotes the cover and management factor (unitless) (Cai et al., 2000), and P is the support practice factor (unitless) (Lufafa et al., 2003). In this study, factors R, K, L, S and C were estimated using the precipitation data in the meteorological site dataset, the soil data in the HWSD database, and the DEM and NDVI data (Table 1). To match the spatial resolution, these data were aggregated into a common spatial resolution of 1 km x1 km for the evaluation of the soil conservation. Then, the values of the soil conservation at 1 km x 1 km

resolution were resampled with respect to municipalities using the module of zonal statistics in ArcGIS 10.0.

$$R = \sum_{i=1}^{12} 1.735 \times 10^{\left(1.5\, lg\left(P_i^2/P\right)-0.08188\right)} \qquad (3)$$

where P_i is the rainfall in month i (mm) and P is the average annual precipitation (mm).

$$K = \left\{0.2 - 0.3exp\left[-0.0256SAN\,\frac{1-SILT}{100}\right]\right\}\left(\frac{SILT}{CLAY+SILT}\right)^{0.3} \times \left[1.0 - \frac{0.25OC}{OC+exp(3.72-2.95OC)}\right] \times \left[1.0 - \frac{0.7\times\left(1-\frac{SAND}{100}\right)}{\left(1-\frac{SAND}{100}\right)+exp\left(-5.51+22.9\times\left(1-\frac{SAND}{100}\right)\right)}\right] \times 0.1317 \qquad (4)$$

where *SAND, SILT, CLAY*, and O*C* are the percentages of sand, silt, clay, and organic carbon, respectively, in the soil and 0.1317 is the conversion coefficient from the US system to the metric system.

$$L = \left(\frac{\lambda}{22.13}\right)^{m} \begin{cases} m = 0.5 & \theta > 9\% \\ m = 0.4 & 3\% < \theta \le 9\% \\ m = 0.3 & 1\% < \theta \le 3\% \\ m = 0.2 & \theta \le 1\% \end{cases} \qquad (5)$$

$$S = \begin{cases} 10.8\sin\theta + 0.03 & \theta < 9\% \\ 16.8\sin\theta - 0.50 & 9\% \le \theta < 18\% \\ 21.91\sin\theta - 0.96 & \theta \ge 18\% \end{cases} \qquad (6)$$

where λ is the slope length (m), m is the slope length index (unitless), and θ is the percentage of the pixel slope that is generated from DEM data.

$$C = \begin{cases} 1, & f = 0 \\ 0.6508 - 0.3436lgf, & 0 < f \le 78.3\% \\ 0, & f > 78.3\% \end{cases} \qquad (7)$$

$$f = \frac{NDVI-NDVI_{min}}{NDVI_{max}-NDVI_{min}} \qquad (8)$$

where *NDVImin* is the minimum NDVI, *NDVImax* is the maximum NDVI, *f* is the degree of vegetation cover, and *C* is the cover and management factor.

In large-scale regions, support practices cannot be identified (Su et al., 2012). The *P* factor was calculated via the empirical methods that utilize the Wiener equation:

$$P = 0.2 + 0.03\alpha \qquad (9)$$

where α is the slope steepness (%) and *P* is the support practice factor.

Carbon sequestration (kilograms of carbon per square kilometer, kg C/km^2): Vegetation provides significant amounts of aboveground foliage for carbon fixation and mediation of the increase in greenhouse gases (Canadell et al., 2007). The net primary production (NPP) can be used as a proxy for carbon sequestration (Peng et al., 2016; Lyu et al., 2019). In this study, NPP was estimated using the process-based Carnegie-Ames-Stanford approach (CASA) model (Potter et al., 1993), which has been widely adopted in NPP estimation (Crabtree et al., 2009). In the model, NPP was driven by vegetation cover, as interpreted from remote sensing images and interpolated maps of climate data in ENVI 5.3 (Gao et al., 2013; Zhou et al., 2017). The equation is expressed as follows:

$$NPP = \sum[APAR(t) \times \varepsilon(t)] \qquad (10)$$

where *NPP* is the net primary productivity (g C/m^2) and *APAR* is absorbed photosynthetically active radiation (MJ/m), which is calculated from the normalized difference vegetation index (NDVI). The MODIS NDVI with 250 m resolution was used in this study (Table 1). The land use/land cover data and NDVI data were integrated into a 1 km $\times$ 1 km resolution. ε is the utilization rate of light energy (g C/MJ) and is affected by the temperature stress, water stress and maximal light utilization efficiency of the vegetation. For additional details, refer to Zhu et al. (2007). The value of NPP per municipality was obtained by allotting the values of NPP at 1 km $\times$ 1 km resolution to municipalities in ArcGIS 10.0.

2.2.3.3. Cultural service

Recreation (number of tourists per square kilometer, person/km^2): The number of

tourists was selected as the proxy for indirect estimation of recreation (Table 2) due to its availability in the areas where other data are scarce, which is in accordance with Bai et al. (2020). The number of tourists for each municipality was obtained from the public statistical yearbooks (Table 1), which included only tourists and not related services such as restaurants.

Table 2

ES indicators from the MA categories and their quantitative methods, units and ES variable requirements. P- Provisioning services, R- Regulating services, and C- Cultural services.

ES indicator	Code	Model or Proxy	Unit	Required ES variable
Crop production	Cro	Crop yield per square kilometer	ton/km^2	Crop yield
Livestock production	Liv	Production of pork, beef and mutton per square kilometer	ton/km^2	Production of pork, beef and mutton
Industrial production	Ind	Gross industrial output value per square kilometer	million yuan/km^2	Gross industrial output value
Water conservation	Wcon	Water storage of the forest ecosystem method as the proxy for the water-conservation service	m^3/km^2	Land use/land cover
Soil conservation	Scon	USLE (universal soil loss equation)	t/(hm^2·a)	Soil database, precipitation, DEM, NDVI, and land use/land cover
Carbon sequestration	Cseq	CASA (Carnegie-Ames-Stanford approach)	kg C/km^2	Land use/land cover, meteorological data, and NDVI
Recreation	Rec	Tourists per square kilometer	persons/km^2	Number of tourists in each municipality

2.2.4. Specialization of ESs

The ES values were individually summarized within each municipality and subsequently standardized to reduce the impacts of the magnitude and variability (Spake et al., 2017). Min-max normalization was used to standardize the ES values by subtracting the minimum value from the ES values of the municipalities and dividing by the difference between the maximum and the minimum values to obtain comparable and dimensionless standardized values that ranged from 0 to 1 (Mouchet et al., 2017; Peng et al., 2017), which can remove the units of the input data. Then, the seven ESs were mapped to visualize the spatial distribution across municipalities. Moran's *I* index was employed to assess the spatial autocorrelation of the ES distribution. The calculation equation is as follows:

$$X_s = \frac{X_i - X_{min}}{X_{max} - X_{min}} \quad (11)$$

where X_s is the standardized value, X is the initial value, X_{min} is the minimum value of ES over 65 municipalities, and X_{max} denotes the maximum value of ES.

2.3. Spatial relationships between ESs

2.3.1. Correlation analysis

Correlations of pairwise ESs were quantified by correlation coefficients based on Spearman's rho, which is frequently used to infer the relationships among ESs that are provided by the ecosystem (Mouchet et al., 2014). The correlations were identified using the Spearman rank correlation (r_p), the correlations were considered statistically significant at $p \leq 0.05$ level. The matrix of correlation coefficients was graphed using the "corrgram" package in the R statistical software. According to the normal curve of the

histogram and the standard deviation in the SPSS software, the ES data conform to the normal distribution characteristics.

2.3.2. ES bundles

Raudsepp-Heard et al. (2010) developed a spatially explicit approach for identifying ES bundles, which has been widely adopted in case studies (Turner et al., 2014; Renard et al., 2015; Spake et al., 2017; Quintas-Soriano et al., 2019). In this approach, principal component analysis (PCA) was used to assess whether ES co-occurs in spatial bundles, and clustering algorithms (K-means cluster) were applied to define groups of ESs that are significantly associated according to the relevant PCA axes. To visualize the ES bundles, the clustering results of the ESs were mapped and the ES values in each ES bundle were represented using spider diagrams or flower plots.

In this study, a three-step approach was employed to delineate ES bundles (ESBs) in this study. First, PCA was used to obtain the principal components (PCs) and a more stable clustering solution (Hanspach et al., 2014; Turner et al., 2014). The numbers of PCs were determined using a scree test and the cumulative variance contribution rate (Qiu and Turner, 2013). A correlation biplot with the relevant PCs as axes was established according to the Kaiser-Guttman criterion (Legendre and Legendre, 2012). In the second step, K-means clustering was applied to the relevant PC axes, which represented 93% of the total variance, to delineate the ES bundles using 1000 random starts and 10,000 iterations. In this way, the K-means clustering municipalities of ES values are more alike within than between clusters. The optimal number of clusters was qualitatively determined by examining the silhouette measure (Schripke et al., 2019). The third step was to import

the cluster resulting values for each municipality into the property sheet of the municipal map in ArcGIS 10.0 to present the spatial distribution of the ES bundles, and flower diagrams were used to illustrate the relative delivery of ESs within each bundle using the R statistical software. These visualizations enabled researchers to identify the localities that exhibit similar relationships between the ESs and to qualitatively interpret them by association with broad socioecological systems (Raudsepp-Hearne et al., 2010; Mouchet et a., 2017).

2.4. Socioecological drivers for ES relationships

2.4.1. Identification of critical driving variables

In selecting the potential driving variables, it was important to include ecological and socioeconomic variables that operate simultaneously (Kienast et al., 2015). In this study, the potential driving variables were selected from (i) the variables that were used in the quantification of the ESs in this study (which include the elevation, slope, climatic variables, and land use/land cover, among others); (ii) the variables that directly or indirectly drive individual ES and/or their associations, as identified in the relative literature (the distance to the nearest city center, the distance to the nearest county center, and the distance to nearest river) (e.g., Peng et al., 2016; Lyn et al., 2019); and (iii) the variables for which quantitative data were available. Thus, thirteen potential driver variables that were important in determining the ES were selected in this study (Table 3).

The land use/land cover and population density have been identified as driving variables of the magnitude and distribution of individual ES and ES bundles (Li et al., 2016; Jaligot et al., 2019). The urban population proportion has been used as an explanatory

variable to analyze the impact of urbanization on the spatial relationship among ESs (Peng et al., 2016). The gross domestic product (GDP) density has been used as an independent variable to identify the response threshold of ES to urbanization (Peng et al., 2017). The distance to the city center and the distance to the county center were used as proxies for urban land expansion. The expansion of urban areas shortens the distance to the wild land that provides provisioning and regulating services, which may affect the provision of ecosystem goods and services (Lyn et al., 2019). It has been shown that the further away from a river, the higher the probability of multiple ES availability (Peng et al., 2016).

Table 3

Details of potential driving variables that are important for ES relationships in this study.

Socioecological variable	Code	Description	Unit	Data source
Elevation	elev	Derived from the SRTM3 global digital elevation model	Meter	NASA
Slope	slop	Derived from the SRTM3 global digital elevation model	Degree	NASA
Precipitation	pre	Annual trends of precipitation for the 1956-2017 period	mm	CMA
NDVI	NDVI	Vegetation cover	%	MODIS
Cropland	crop	Municipality land area that is occupied by area that is classified as cropland	%	RESDC
Forestland	forest	Municipality land area that is occupied by area that is classified as forest	%	RESDC
Grassland	grass	Municipality land area that is occupied by area that is classified as grassland	%	RESDC

Bare land	bare	Municipality land area that is occupied by area that is classified as bare land	%	RESDC
Population density	pop	Population density per square kilometer, as obtained by dividing the municipality population size by its area	person/km^2	NBSC
Urbanization rate	urban	Urban population proportion	%	NBSC
Economic level	GDP	Gross domestic product density	yuan/km^2	NBSC
Distance to the city center	city	European distance to the nearest city center	km	NGCC
Distance to the county center	county	European distance to the nearest county center	km	NGCC
Distance to the river	river	European distance to the nearest river	km	NGCC

To identify the candidate driving variables that significant affect the ESs, a redundancy analysis (RDA) with all the potential driving variables and a forward stepwise procedure were conducted to select the model with the combination of variables with the highest R^2 value and the smallest p-value (Legendre and Legendre, 2012) using the "vegan" and "packfor" packages in R. RDA revealed that the combinations of the following variables significantly explained the ESs in the YRB ($p \leq 0.001$): slope, precipitation, crop land, forestland, grass land, bare land, population density, urbanization rate, economic density and distance to the river. Linear dependencies among the driving variables were further explored by computing the variation inflation factors (VIFs). All the VIF values were below 5; hence, the multicollinearity of the variables was not problematic in the models. Subsequently, the significant socioecological variables were mapped. According to the spatial resolution of the primary data of the socioecological variables, the population density, urbanization rate and economic density, along with the municipality, slope,

precipitation, crop land, forestland, grass land and bare land, were mapped with a resolution of 1 km x1 km. Spatial raster data of the distance to the river with a resolution of 1 km x1 km are obtained by using the river as a buffer. These driving variables were normalized using the min-max normalization to render them comparable and consistent with the ESs and ES bundles as the dependent variables.

2.4.2. Effects of individual driving variables on the ES distribution

The spatial distribution of an ES may be closely associated with multiple driving variables simultaneously. In the study area, the formation of each ES spatial pattern is the result of the spatial superposition of multiple driving variables. It is difficult to distinguish the contribution of each factor to the spatial patterns of ESs in the superposition process. The geo-detector model (GDM) was used to detect the effects of individual driving variables on the ES distribution because it has advantages in terms of spatial stratification, heterogeneity, and categorical variables.

The GDM was applied mainly to assess the spatial correlation between the explaining variables and the explained variables via spatial variance analysis (SVA) (Wang et al., 2010; Wang et al., 2016). The core strategy of the GDM is based on the following assumption: if an independent variable X has a significant effect on a dependent variable Y, then the spatial distributions of the independent variable and the dependent variable should be similar (Hu et al., 2011). GDM has unique advantages in dealing with both numerical and categorical variables and has been used to detect the effects of socioecological drivers on the spatial distribution of ESs (Lyu et al., 2019; Chen et al., 2020). In this study, the “factor detector” module of GDM was used to detect the spatial

effect of each driving variable on the ESs by detecting the extent to which socioecological drivers explain the spatial differentiation of the ES (Wang et al., 2010). The calculation results of the factor detector include the *q*-statistic and *p*-value. The *q*-statistic is the influencing coefficient of the driving variable on the ES. The larger the *q*-statistic is, the stronger the impact of the socioecological driver on the ES. The *p*-value indicates the significance level of the explanation, and significance is determined the 0.1 level (*p*-value < 0.1). The exploration of the association between the driving variables and the ES is expressed as follows:

$$q = 1 - \frac{\sum_{h=1}^{L} N_h \sigma_h^2}{N\sigma^2} \quad (12)$$

where *q* signifies the influencing coefficients of the driving variables for the ES (*q*-statistic), the values of which range from 0 to 1, namely, 0 corresponds to no correlation between the two and 1 to the ES's complete dependence on a driving variable; σ^2 is the variance of the ES; and *N* is the size of the ES. The superposition of the driving variables and the ES forms *L* layers in the ES, which are indexed by *h* = 1, 2.. l, and N_h and σ_h^2 represent the scale and variance, respectively, of layer *h*.

2.4.3. Spatial overlay of ES bundles and social-ecological clusters

Based on the most important socioecological determinants of ESs that were identified using RDA, PCA and the K-means algorithm were used to cluster these driving variables into socioecological clusters (SECs) by following the procedure that is suggested in Section 2.3.2. To assess whether the ESBs are spatially associated with SECs, the spatial congruence between them was assessed using the spatial overlap. Then, the percentage of municipalities of each ESB that overlapped with each SEC category was calculated.

3. Results

3.1. Spatial distribution of ESs

The provision of the seven ESs varied substantially across the YRB and exhibited spatial autocorrelation (Moran's $I \geq 0.34$, $p = 0.000$) (Table 4). The areas with the maximum values of crop production, livestock production, and industrial production were most prominent in the eastern plains of the YRB (Fig. 2). The water conservation was distributed dispersedly across the southern parts. High-value areas of water conservation were found in the Yushu Tibetan Autonomous Prefecture in the Qinghai-Tibet Plateau, Baoji and Xi'an in the Qinling Mountains. The high-value areas of soil conservation were also observed in the Qinling Mountains, whereas the low-value areas were found in the northern parts (where desert was the main land cover type) and the eastern plains. The high-value areas of carbon sequestration were concentrated primarily in the southern mountainous parts and the eastern plains. The low-value areas were primarily in the northern Loess Plateau and western Qinghai-Tibet Plateau. The provision of recreation was higher in the southeastern parts with more densely populated municipalities and was lower in the other regions of the study area. Overall, the distributions of provisioning and cultural services exhibited readily observable east-west differences, and regulating services showed an observable south-north difference.

Table 4

Global spatial autocorrelation index of ES indicators (Moran's *I*)

ES indicator	Moran's *I*	*p* significance value

Crop production	0.57	0.000000
Livestock production	0.67	0.000000
Industry production	0.40	0.000000
Water conservation	0.31	0.000000
Soil conservation	0.53	0.000000
Carbon sequestration	0.66	0.000000
Recreation	0.35	0.000000

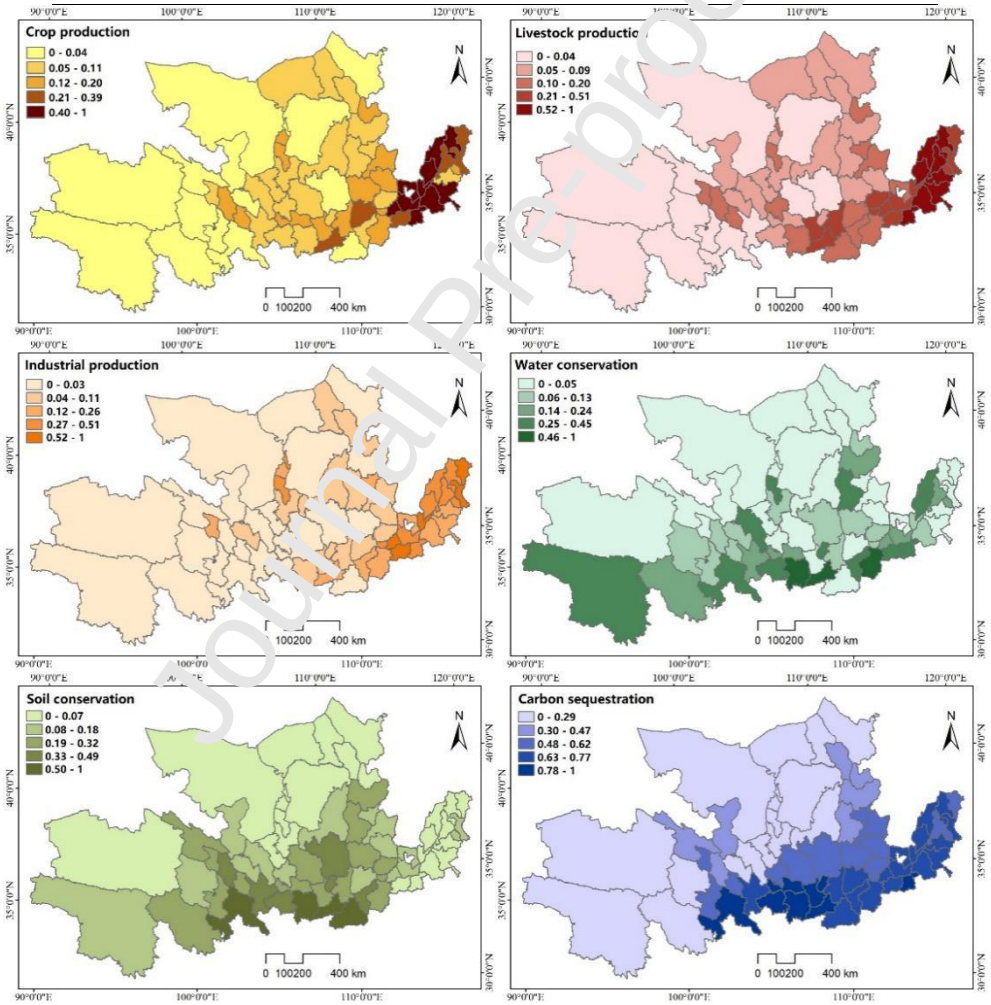

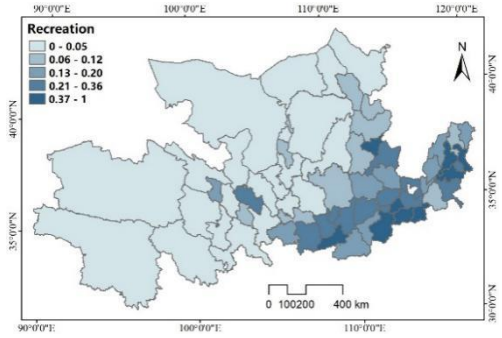

Fig. 2. Spatial distributions of the ESs across the 65 municipalities in the YRB.

3.2. Trade-offs and synergies among ESs

The negative and positive correlation pairs of ESs highlighted the trade-off and synergistic relations across the study area (Fig. 3). Among the 21 pairs of ESs, 17 significantly correlated pairs between ESs ($p \leq 0.05$), a total of 14 were positively correlated, and the remaining 3 were negatively correlated. Additionally, 1 of them were highly correlated (*Pearson coefficient*, $r \geq 0.7$), a total of 4 were moderately correlated ($0.5 \leq r < 0.7$), and 12 was weakly correlated ($r < 0.7$). The provisioning services had the strongest positive correlations with each other, while they were negatively correlated with soil conservation. Soil conservation, which depends strongly on regulating services through vegetation cover, was highly positively correlated with water conservation and carbon sequestration. Water conservation was also positively correlated with carbon sequestration recreation but was not significantly correlated with provisioning services. Carbon sequestration was significantly positively correlated with provisioning, regulating and cultural services. Recreation was positively correlated with all other services except soil conservation.

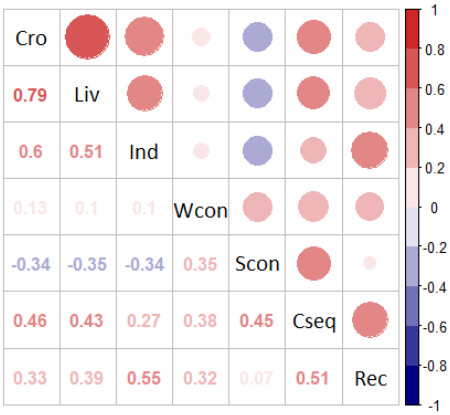

Fig. 3. Spearman's rank correlation coefficients of pairs of ESs in the YRB. The darker the color of the correlation coefficient font, the higher the significance level. The correlations were considered statistically significant at $p \leq 0.05$ level. Cro: crop production; Liv: livestock production; Ind: industrial production; Wcon: water conservation; Scon: soil conservation; Cseq: carbon sequestration; and Rec: recreation.

3.3. Spatial distribution and characteristics of ES bundles

Two principal components that explained 70.28% of the variance of ESs were identified by PCA across the study area (Fig. 4). The first principal component axis (PC 1) represented a trade-off between soil conservation and most other services, most strongly with crop production. The second principal component axis (PC 2) represented a synergy among crop production, livestock production and industrial production and their trade-offs with soil conservation. The 65 municipalities were partitioned into three groups of ES bundles via K-means clustering based on the types and amounts of ESs (Fig. 5). The number of municipalities in each bundle varied from 14 to 36. The bundles were named based on the dominant ES, land cover and the socioecological characteristics.

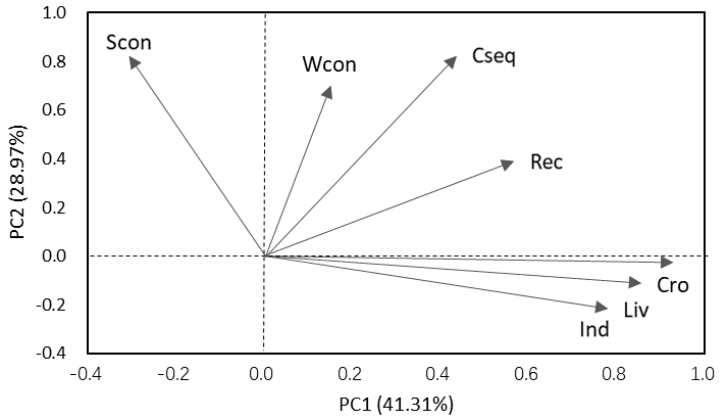

Fig. 4. The principal component analysis biplot for ESs in the YRB. Cro: crop production; Liv: livestock production; Ind: industrial production; Wcon: water conservation; Scon: soil conservation; Cseq: carbon sequestration; and Rec: recreation.

The **agricultural bundle** (ESB 1, n = 15) covered 6.3% of the study area. This bundle clustered in the most important agricultural cultivation region in the eastern YRB (Fig. 5 a). It was comprised of municipalities that were characterized by the highest values of crop production, livestock production and industrial production (Fig. 5 b). The potential for water conservation and soil conservation was very low. This bundle had the highest value for recreation. The **forest regulation bundle** (ESB 2, n = 14) covered 12.3% of the study area. It was comprised of municipalities that had high values for regulating services and a moderate value for recreation but relatively low values for provisioning services (Fig. 5 b). An ESB with a relatively single provision of carbon sequestration was identified, namely, a **grassland and desert bundle** (ESB 3, n = 36), the ESs of which were distributed widely across arid and semiarid areas with the highest proportion of bare land and grassland (Table 5). It covered 81.4% of the study area and had the largest number of municipalities, and it occupied the medium- and high-altitude areas (Fig. 5 a, Fig. 1 c). Carbon sequestration was much higher than other ESs in this bundle, while it was much lower

than the carbon sequestration values in ESB 1 and ESB 2 (Fig. 5 b).

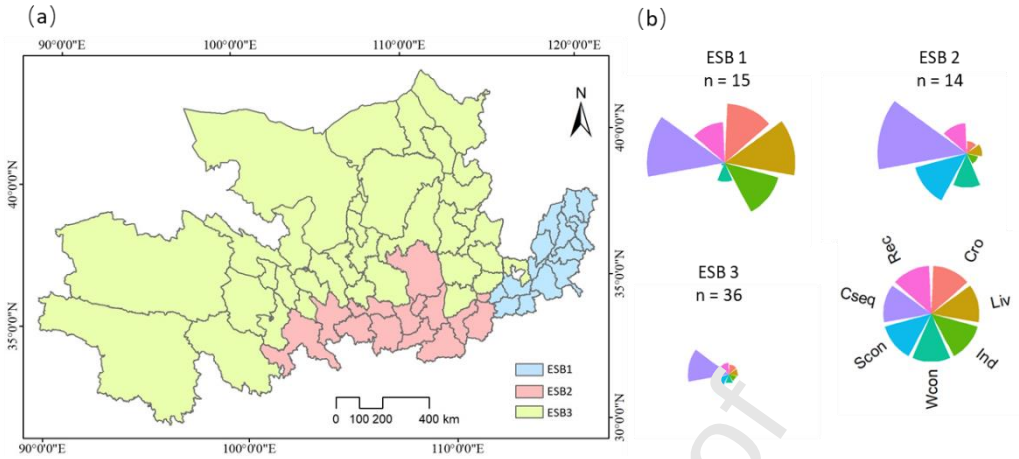

Fig. 5. Spatial distribution of the ES bundles that were identified via K means clustering for the study area. n is the number of municipalities that are grouped in each bundle. The flower diagrams are dimensionless and are based on normalized data for each service. The lengths of the petals are comparable within each bundle and among bundles. Cro: crop production; Liv: livestock production; Ind: industrial production; Wcon: water conservation; Scon: soil conservation; Cseq: carbon sequestration; and Rec: recreation.

Table 5

Area proportions of land use/land cover types in each ESB (%).

ES bundle	Cropland	Forestland	Grassland	Wetland	Water	Impervious surface	Bare land	Snow/Ice
ESB 1	74.87	4.62	1.85	0.21	3.90	13.59	0.30	0.00
ESB 2	29.01	41.78	24.92	0.07	0.41	2.51	0.43	0.01
ESB 3	9.87	4.61	34.36	0.19	1.29	1.61	47.21	0.46

3.4. Determining socioecological drivers for ESs

The detection results for 10 socioecological variables were obtained through the factor detectors of GDM, which include the influencing coefficients (q-statistic values) of

the ESs and the degree of significance (*p*-value) (Table S1). Fig. 6 presents the *q*-statistic value of each socioecological variable to reveal their influencing coefficients on individual ESs. For crop production and livestock production, the influencing coefficients can be ranked according to the *q*-statistic as cropland (0.73) > population density (0.60) > slope (0.53) > GDP (0.50). This result demonstrates that the determinate drivers of these two services were similar. GDP had the largest influencing coefficients for industrial production. Water conservation was influenced mainly by precipitation, although the influencing coefficient was only 0.24. Slope and forestland were the determinate variables of soil conservation according to the *q*-statistic value. Six socioecological variables had larger influencing coefficients for carbon sequestration: bare land (0.72), precipitation (0.63), distance to river (0.50), population density (0.39), forestland (0.39) and cropland (0.37). For recreation, GDP (0.71) and population density (0.59) were the major determinants.

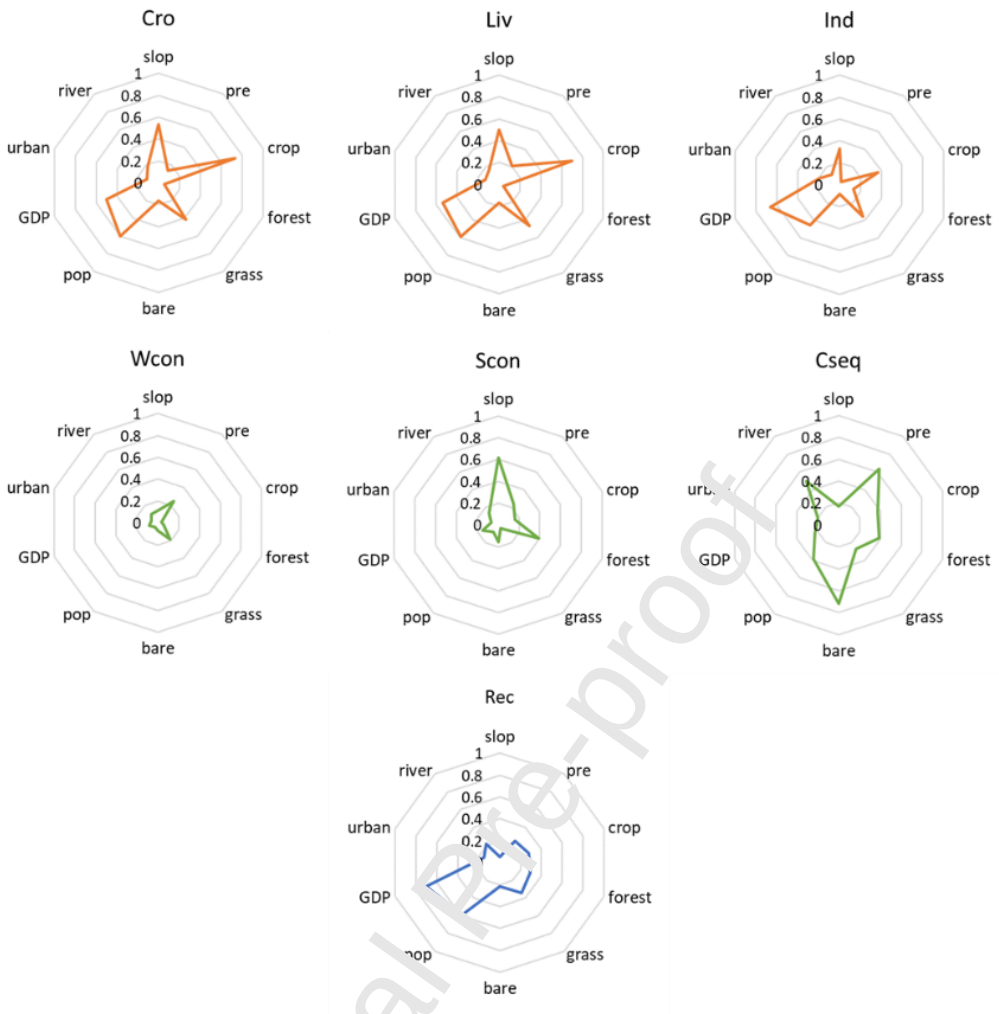

Fig. 6. Factor-detected results of determinants of ESs using GDM. The values on the axis of each radar diagram represent the *q*-statistic values. The orange broken lines correspond to provisioning services, the green broken lines correspond to regulating services and the blue broken line corresponds to the cultural service. slop: slope; pre: precipitation; crop: cropland; forest: forestland; grass; grassland; bare: bare land; pop: population density; urban: urbanization rate; GDP: economic density; and river: distance to the river.

3.5. Characterization of ES bundles by socioecological covariates

The 65 municipalities were grouped and partitioned into four clusters according to 10 social-ecological driving variables. The distributions of the four SECs presented spatial differences throughout the study area (Fig. 7 a). The results of the spatial overlay (Fig. 8)

demonstrated that ESB 1 (Fig. 5) was dominated by provisioning services (Fig. 6 b) and co-occurred spatially with SEC 4 (100%), which was determined by the cropland, precipitation, and socioeconomic variables (Fig. 7 b). ESB 2, for which the importance of regulating services was high (Fig. 6 b), was mapped mainly in the areas of SEC 3 (85.4%) (Fig. 8) and was characterized by large values for the ecological variables and the urbanization rate (Fig. 7 b). Sorted in descending order of the percentage of overlap area of each cluster, ESB 3 overlapped with SEC 2 (64%), SEC 1 (22.2%), and SEC 3 (12.2%) (Fig. 8), which were determined synthetically from ecological and socioeconomic variables. SEC 2 was characterized by large values for bare land and grassland, and SEC 1 was characterized by the largest values for grassland and slope (Fig. 7 b).

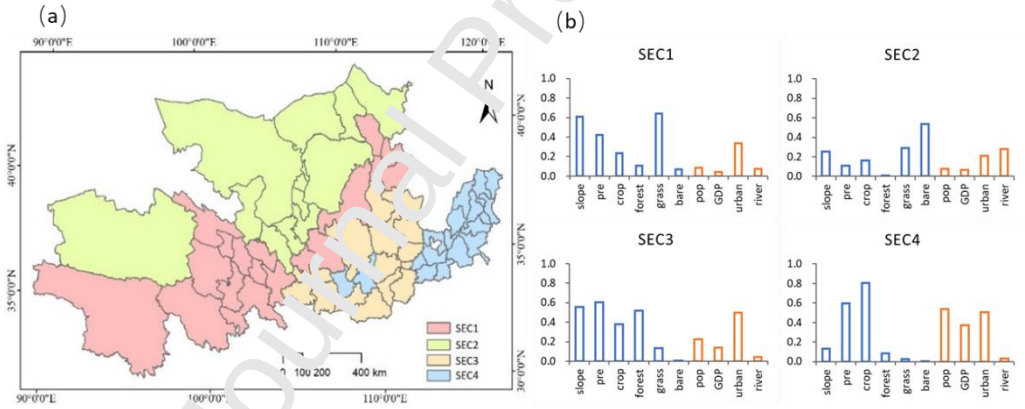

Fig. 7. Social-ecological clusters (SECs) that are mapped in the study area: (a) The spatial distribution of four SECs and (b) bar graphs that are based on normalized data for each socioecological driving variable, in which the height of each bar corresponds to the contribution of each variable to the clusters. The SEC areas are dominated by either ecological (blue) or socioeconomic (orange) covariates. slop: slope; pre: precipitation; crop: cropland; forest: forestland; grass: grassland; bare: bare land; pop: population density; urban: urbanization rate; GDP: economic density; and river: distance to the river.

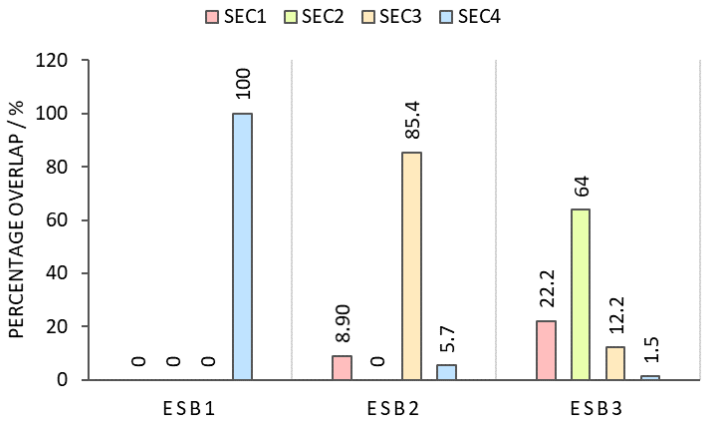

Fig. 8. Overlap of each ES bundle (ESB) per socioecological cluster (SEB) in % of area in the YRB.

4. Discussion

4.1. Trade-offs and synergies among ESs with socioecological covariates

The synergies between paired ESs substantially exceeded the trade-offs in this study (Fig. 3 a). The strongest synergetic relation was observed between crop production and livestock production (Fig. 3 a), which was consistent with previous studies (Raudsepp-Hearne et al., 2010; Yang et al., 2015). This might be explained by their similar primary determinants, namely, cropland and population density, with the highest influencing coefficients in the detection results of GDM (Fig. 6). Bennett et al. (2009) proposed that the provision of ESs can be related either to interactions between ESs or to responding to the same drivers. As presented in Fig. 2 and Table 4, the spatial patterns of the provision of crop production and livestock production were similar. Thus, it was suggested that the strong synergic relation between crop production and livestock production depended on the positive responses to the same determinants. Surprisingly, synergies were identified between recreation and all other services except soil

conservation. The main reason was that recreation was related mainly to socioeconomic variables (Fig. 6) and did not require as much land as provisioning and regulating services (Peng et al., 2016). For instance, various agricultural or forest landscapes can also be used as leisure spaces to attract tourists (Yang et al., 2015; Peng et al., 2016).

Trade-off relations were identified between provisioning services and soil conservation in the correlation analysis results among the ESs (Fig. 3 a). This was consistent with the results from previous studies (Raudsepp-Hearne et al., 2010; Chen et al., 2020). The determining drivers of soil conservation were slope and forestland (Fig. 6). Hence, the high provision areas of soil conservation contained substantial forest cover. However, there is land use competition between forestland and cropland, which depended heavily on the provision of provisioning services. Therefore, these trade-offs might be caused by spatial incompatibilities that are due to the dependence of provisioning and regulating services on the associated land-use types in this study.

4.2. Spatial distribution and characteristics of ES bundles

The detected agricultural bundle was characterized mostly by crop and livestock production (Fig. 5 b), which supported the findings of previous studies on ESBs (Raudsepp-Hearne et al., 2010; Turner et al., 2014; Yang et al., 2015; Spake et al., 2017), such as the corn-soy bundle in Quebec, the agriculture bundle in Denmark and the plain-city bundle in the Yangtze River Delta. This bundle was distributed on the flattest plains of the downstream region of the YRB (Fig. 1, Fig. 5 a), and cropland accounted for as much as 74.87% (Table 5). This regional concentration of provisioning services likely reflects the ongoing specialization in agricultural production, which is also occurring for

other regions, as shown by Dittrich et al. (2017). A forest regulation bundle was identified in the mixed forested and cropland areas that belong to the transitional mountains between the cropland plains and the grassland mid-elevation plateau (Fig. 1, Fig. 5 a). The proportion of forest in this bundle area was the highest among the three ESBs (Table 5). As shown in Fig. 5 b, ESB 2 had a large value for the regulating services, which agreed well with previous results (e.g., Raudsepp-Hearne et al., 2010), according to which the large values of regulating services were often related to substantial forest cover. This supported the findings of Buyantuyev et al., (2009) that the carbon sequestration that was provided by desert and grassland was lower than that by forest and cropland when accounting for NPP as the proxy method. Additionally, trade-offs with distinct signs were identified between provisioning services and soil conservation and water conservation in the agricultural bundle and the forest regulation bundle (Fig. 5 b). This supported a common finding that trade-offs dominated the relationships between provisioning and regulating services (Rodríguez et al., 2006; Lee and Lautenbach, 2016).

4.3. Associations between ES bundles and socioecological covariates

It was found that the agricultural bundle mainly overlapped with SEC 4 due to the large values for cropland and precipitation and the socioeconomic conditions (Fig. 7, Fig. 8). This highlighted the importance of the amount of cropland and the population density for provisioning services. This result was supported by other studies (Qiu and Turner, 2013; Jaligot et al., 2019) that showed that cropland and population density variables were the determinants of the distribution of provisioning services. Nevertheless, the agricultural bundle regional concentration of this study was distributed in the

high-population-density area (Fig. 1, Fig. 5 a), which was inconsistent with the results of Turner et al. (2014), who identified the largest values of crop and livestock production in the less populated areas. One explanation could be that the agricultural practices were more intensive in Danish municipalities that were under high agricultural land-use pressure than in the agricultural bundle area in this study, especially for crop and pork production.

In contrast, the forest regulation bundle that was dominated by regulating services overlapped mainly with the intermediate SEC 3 due to the large values for precipitation and forestland (Fig. 7 b, Fig. 8). This was consistent with a finding of Spake et al. (2017) in a French Alps case study that the ESB that was dominated by regulating services in the southern Alps overlapped mainly with forest cover. In this study, the high forest cover in this bundle area might be explained by the coupled effects of natural conditions and human intervention. This bundle was distributed in the northern margin of Qinling mountain with abundant rainfall (Fig. 1), which corresponded to the natural predominance of high forest cover. In terms of human intervention, a series of ecological restoration programs have been implemented to mitigate the degradation of water and for soil conservation since 1999 (Su et al., 2012; Jiang et al., 2016). The Grain for Green Project (GFGP), which targets the conversion of cropland to forest and grassland, positively affected the forest-dominated ESs in this bundle area (Li et al., 2016; Jiang et al., 2017).

The grassland and desert bundle overlapped widely with three SECs (SEC 2, SEC 1, and SEC 3), which were determined largely by ecological variables (Fig. 7 b and Fig. 8). According to the average values of the socioecological variables, these three SECs were

ranked as SEC 2, SEC 1, and SEC 3 (Fig. 7 b), and the primary determinants of this bundle were grassland and bare land. This can be explained by the observation that this bundle was covered mainly by widespread grassland and bare land (Fig. 1 and Fig. 7 a), which accounted for 40.8% and 49.3%, respectively, of the total area of this bundle. In this case, the absence of pronounced socioeconomic gradients may have limited the diversity of the ESs and, thus, prevented known trade-offs with provisioning and cultural services.

4.4. Limitations

This study has limitations in the quantification of ESs due to poor data availability. The sensitivity of ES relationships depends on the indicator selection and accuracy of ES quantifications (Liu et al., 2017). Although the selected ES indicators depended on the ecosystems for their provision and were relevant to the study areas, the availability and quality of the data severely limited the set of ESs that we could use. To accurately quantify the ESs, we considered the ES variables for which spatial, statistical and text data were all available for the study area and the assessment accuracies of the models (De Groot et al., 2010; Mouchet et al., 2014; Lee and Lautenbach, 2016). When evaluating the ESs, more than one proxy-based model was used in this study, which inevitably generated uncertainties regarding data collection or parameter selection. For instance, the calculation of the proxy model for water conservation depends on the secondary type and area of the forest. Although this approach had been applied by Yang et al. (2015) in the Yangtze River Delta to estimate water conservation, a type of LULC may not have the same ES value for all sites, as in this and previous studies (Turner et al., 2014). For the soil conservation, the evaluation results of USLE were less accurate in the situations,

where the terrain is more complex, tillage systems vary at small scales, and tillage and management practices are not specificity. In addition, the number of tourists was used as the proxy variable for evaluating recreation (Bai et al., 2020), which likely led to overestimation. However, the official statistics on tourists of each municipality were publicly accessible, which enabled the direct measurement of the utility of ESs and ES mapping in data-scarce regions (Meacham et al., 2016).

LULC has been regarded as an important determinant of ESs or ES bundles in this study and many others (Haman et al., 2015; Meacham et al. 2016; Schulze et al., 2016; Dade et al., 2018; Ndong et al., 2020).

The LULC categories were treated as homogeneous across the study units in this study, and the variations of LULC that were due to management practice and biophysical gradients were ignored (Spake et al., 2017). Moreover, coarse descriptors such as the proportions of cropland, forest, grassland, and bare land were used as the LULC driver variables, and only the data availability of land variables in the YRB was considered. Neither land use nor management practices (Lyu et al., 2019) were considered in the socioecological variables. Indeed, it has been suggested that land use and management (e.g., agricultural practices) constitute the basis of service provision (De Groot et al., 2010). The unmeasured variables or practices could affect trade-offs, synergies, and ES bundles in the study area (Spake et al., 2017). Therefore, we agreed with Burkhard et al. (2012) on the necessity of identifying the effects of management practices on ESs for optimal ecosystem management.

The administrative boundaries that were used in this study were advantageous for

obtaining official statistical data and providing management decisions. However, the municipal spatial unit was cruder (Raudsepp-Hearne and Peterson, 2016), and understanding of the causality in ES relationships was limited (Cord et al., 2017). In this study, the average municipality area was 27,979 km2 and ranged from 1,656 to 253,015 km2. To reduce the scale effects of the variation of the spatial unit area, the ES indicator and socioecological variables that were related to the municipal area were quantified by dividing by the area. However, the area of the spatial units in this study was much larger than those in previous studies that applied the same ES bundle approach (e.g., Raudsepp-Hearne et al., 2010; Yang et al., 2015; Queiroz et al., 2015; Spake et al., 2017; Jaligot R et al., 2019; Quintas-Soriano et al., 2019). This approach failed to represent the fine-grained ecological and artificial aspects in such large space units, which were especially important for the formation and consequence determination of the ES bundles (Burkhard et al., 2012). Therefore, the ES bundles should be delineated at multiple spatial grain sizes, including municipalities, across the study area in future studies.

5. Conclusions

This study assessed the spatial relationships (trade-offs, synergies, and bundles) among multiple ESs and identified their social-ecological driving factors. The results presented spatial differences in ESs and their statistical correlations at the regional scale. Crop production, livestock production, and industrial production were synergistic with one another and were determined by similar driving variables: cropland and population density. These provisioning services all had trade-off relationships with soil conservation.

Surprisingly, the synergies between ESs well exceeded the trade-offs in the study area. Three ES bundles were detected among the seven ESs. In the eastern wide plains, the ecosystem provided a high provision of provisioning services, which was strongly driven by cropland, precipitation and socioeconomic variables. In the southeastern transitional mountains between the cropland plains and the grassland, the ecosystem was characterized by a high provision of regulating services, which was driven mainly by high forest cover. In the western and northern parts of the YRB, all the limited ESs were supplied except carbon sequestration, which was mainly determined by grassland and bare land. It was observed that LULC plays major roles in the spatial distribution of ESBs and in the trade-offs and synergies between ESs within each ESB. This study provides a comprehensive analysis of ES relationships and their socioecological drivers across the YRB in a large-scale basin. In the future, it is critical to focus on suitable sustainable management strategies according to the similar composite patterns of ES bundles and social-ecological drivers.

Acknowledgements

This research was funded by the National Natural Science Foundation of China under grant No. 41771128 and 41671176, the Ministry of Education of Humanities and Social Science Project under grant No. 19YJA890006 and Liaoning Revitalization Talents Program under grant No. XLYC1807060. We thank the academic editors and anonymous reviewers for their kind suggestions and valuable comments.

References

Bai, Y., Zhuang, C., Ouyang, Z., Zheng, H., Jiang, B., 2011. Spatial characteristics between biodiversity and ecosystem services in a human-dominated watershed. Ecological Complexity. 8, 177-183. http://dx.doi.org/10.1016/j.ecocom.2011.01.007.

Bai, Y., Chen, Y.Y., Alatalo, J.M., Yang, Z.Q., Jiang, B., 2020. Scale effects on the relationships between land characteristics and ecosystem services- a case study in Taihu Lake Basin, China. Sci Total Environ. 716, 137083. https://doi.org/10.1016/j.scitotenv.2020.137083.

Bennett, E.M., Peterson, G.D., Gordon, L.J., 2009. Understanding relationships among multiple ecosystem services. Ecol Lett. 12, 1394-1404. https://doi.org/10.1111/j.1461-0248.2009.01387.x.

Bennett, E.M., Cramer, W., Begossi, A., Cundill, G., Díaz, S., Egoh, B.N., Hebel, L., 2015. Linking biodiversity, ecosystem services, and human well-being: three challenges for designing research for sustainability. Curr Opin Environ Sustain. 14, 76-85. https://doi.org/10.1016/j.cosust.2015.03.007.

Bing, L.F., Shao, Q.Q., Liu, J.Y., Zhao, Z.P., 2011. Runoff characteristic in flood and dry seasons in source regions of Changjiang River and Huanghe River based on wavelet analysis. Sci. Geogr. Sin. 31, 2323-2328. https://doi.org/10.13249/j.cnki.sgs.2011.02.016.

Brauman, K.A., Daily, G.C., Duarte, T.K., Mooney, H.A., 2007. Thenature and value of ecosystem services: An overview highlighting hydro-logic services. Annual Review of Environment and Resources. 32, 67-98. http://dx.doi.org/10.1146/annurev.energy.32.031306.102758.

Burkhard, B., Kroll, F., Nedkov, S., Muller, F., 2012. Mapping ecosystem service supply, demand and budgets. Ecol. Indic. 21, 17-29. https://doi.org/10.1016/j.ecolind.2011.06.019.

Buyantuyev, A., Wu, J., 2009. Urbanization alters spatiotemporal patterns of ecosystem primary production: A case study of the Phoenix metropolitan region, USA. J. Arid. Environ. 73, 512-520. https://doi.org/10.1016/j.jaridenv.2008.12.015.

Cai, C., Ding, S.W., Shi, Z.H., Huang, L., Zhang, G.Y., 2000. Study of applying USLE and geographical information system IDRISI to predict soil erosion in small watershed. J. Soil Water Conserv. 14, 19-24.

Canadell, J.G., Le Quere, C., Raupach, M.R., Field, C.B., Buitenhuis, E.T., Ciais, P., Conway, T.J., Gillett, N.P., Houghton R.A., Narland, G., 2007. Contributions to accelerating atmospheric CO^2 growth from economic activity, carbon intensity,

and efficiency of natural sinks. Proc. Natl. Acad. Sci. U.S.A. 104(47), 18866-18870. https://doi.org/10.1073/pnas.0702737104.

Chen, T.Q., Feng, Z., Zhao, H., Wu, K.N., 2020. Identification of ecosystem service bundles and driving factors in Beijing and its surrounding areas. Sci Total Environ. 711, 134687-194702. https://doi.org/10.1016/j.scitotenv.2019.134687.

Chi, Y., Shi, H.H., Zheng, W., Sun, J.K., Fu, Z.Y., 2018. Spatiotemporal characteristics and ecological effects of the human interference index of the Yellow River Delta in the last 30 years. Ecol. Indic. 89, 880-92. https://doi.org/10.1016/j.ecolind.2017.12.025.

Cord, A.F., Bartkowski, B., Beckmann, M., et al., 2017. Towards systematic analyses of ecosystem service trade-offs and synergies: main concepts, methods and the road ahead. Ecosyst. Serv. 28, 264-272. https://doi.org/10.1016/j.ecoser.2017.07.012.

Costanza, R., dArge, R., deGroot, R., et al., 1997. The value of the world's ecosystem services and natural capital. Nature. 387, 253-260. https://doi.org/10.1016/S0921-8009(98)00020-2.

Crabtree, R., et al., 2009. A modeling and spatio-temporal analysis framework for monitoring environmental change using NPP as an ecosystem indicator. Remote Sens. Environ. 113, 1486-1496. http://dx.doi.org/10.1016/j.rse.2008.12.014.

Crouzat, E., Mouchet, M., Turkelboom, F., Byczek, C., Meersmans, J., Berger, F., Verkerk, P.J., Lavorel, S., 2015. Assessing bundles of ecosystem services from regional to landscape scale: insights from the French Alps. J. Appl. Ecol. 52, 1145-1155. https://doi.org/10.1111/1365-2664.12502.

Dade, M.C., Mitchell, M.G., McAlpine, C.A., Rhodes, J.R., 2018. Assessing ecosystem service trade-offs and synergies: the need for a more mechanistic approach. Ambio. 48, 1116-1128. https://doi.org/10.1007/s13280-018-1127-7.

De, Groot, R.S., Alkemade, R., Braat, L., Hein, L., Willemen, L., Challenges in integrating the concept of ecosystem services and values in landscape planning, management and decision making. Ecol. Complex. 7, 260-272. https://doi.org/10.1016/j.ecocom.2009.10.006.

Dittrich, A., Seppelt, R., Václavík, T., Cord, A.F., 2017. Integrating ecosystem service bundles and socio-environmental conditions - a national scale analysis from Germany. Ecosyst Serv. 28, 273-282. https://doi.org/10.1016/j.ecoser.2017.08.007.

Feng, Q., Zhao, W., Fu, B., Ding, J., Wang, S., 2017. Ecosystem service trade-offs and their influencing factors: A case study in the loess plateau of China. Sci Total Environ. 607-608, 1250-1263. https://doi.org/10.1016/j.scitotenv.2017.

Fu, B., Zhang, L., Xu, Z., Zhao, Y., Wei, Y., Skinner, D., 2015. Ecosystem services in changing land use. J. Soils Sediments. 15, 833-843. https://doi.org/10.1007/s11368-015-1082-x.

Gao, Q., Wan, Y., Li, Y., Guo, Y., Ganjurjav, Qin, X., et al., 2013. Effects of topography and human activity on the net primary productivity (NPP) of alpine grassland in northern Tibet from 1981 to 2004. Int J Remote Sens, 34, 2057-2069. https://doi.org/10.1080/01431161.2012.734933.

Gonzalez-Ollauri, A., Mickovski, S.B., 2017. Providing ecosystem services in a challenging environment by dealing with bundles, trade-offs, and synergies. Ecosyst Serv. 28, 261-263. https://doi.org/10.1016/j.ecoser.2017.10.004.

Grimaldi, M., Oszwald, J., Dolédec, S., Hurtado, M.D.P., de Souza Miranda, I., Arnauld de Sartre, X., Assis, W.S.D., Castañeda, E., Desjardins, T., Dubs, F., Guevara, E., Gond, V., Lima, T.T.C., Marichal, R., Michelotti, F., Mitja, D., Noronha, N.C., Delgado Oliveira, M.N., Ramirez, B., Rodriguez, G., Sarrazin, M., Silva, M.L.D., Costa, L.G.S., Souza, S.L.D., Veiga, I., Velasquez, E., Lavelle, P., 2014. Ecosystem services of regulation and support in Amazonian pioneer fronts: searching for landscape drivers. Landscape Ecol. 29, 311-328. https://doi.org/10.1007/s10980-013-9981-y.

Hamann, M., Biggs, R., Reyers, B., 2015. Mapping social-ecological systems: identifying 'green-loop' and 'red-loop' dynamics based on characteristic bundles of ecosystem service use. Global Environmental Change: Human and Policy Dimensions. 34, 218-226. http://dx.doi.org/10.1016/j.gloenvcha.2015.07.008.

Hanspach, J., Hartel, T., Milcu, A.I., Mikulcak, F., Dorresteijn, I., Loos, J., von Wehrden, H., Kuemmerle, T., Abson, D., Kovács-Hostyánszki, A., Báldi, A., Fischer, J., 2014. A holistic approach to studying social-ecological systems and its application to southern Transylvania. Ecol. Soc. 19, 32. https://doi.org/10.5751/ES-06915-190432.

Han, Z., Song, W., Deng, X.Z., Xu, X.L., 2017. Trade-Offs and Synergies in Ecosystem Service within the Three-Rivers Headwater Region, China. Water-Sui. 9, 588. https://doi.org/10.3390/w9080588.

Hu, Y., Wang, J.F., Li, X.H., Ren, D., Zhu, J., 2011. Geographical Detector-Based Risk Assessment of the Under-Five Mortality in the 2008 Wenchuan Earthquake, China. PLoS ONE. 6, 21427. https://doi.org/10.1371/journal.pone.0021427.

Jaligot, R., Chenal, J., Bosch, M., 2019. Assessing spatial temporal patterns of ecosystem services in Switzerland. Landscape Ecol. 34, 1379-94. https://doi.org/10.1007/s10980-019-00850-7.

Jiang, C., Zhang, L.B., 2015. Climate change and its impact on the eco-environment of the Three-Rivers Headwater Region on the Tibetan Plateau, China. Int. J. Environ. Res. Public Health. 12, 12057-12081. https://doi.org/10.3390/ijerph121012057.

Jiang, C., Wang, F., Zhang, H.Y., Dong, X.L., 2016. Quantifying changes in multiple ecosystem services during 2000-2012 on the Loess Plateau, China, as a result of climate variability and ecological restoration. Ecol Eng. 97, 258-271. https://doi.org/10.1016/j.ecoleng.2016.10.030.

Jiang, C., Zhang, L.B., 2016. Ecosystem change assessment in the Three-river Headwater Region, China: Patterns, causes, and implications. Ecol Eng. 93, 24-36. https://doi.org/10.1016/j.ecoleng.2016.05.011.

Jiang, C., Zhang, H.Y., Zhang, Z.D., 2018. Spatially explicit assessment of ecosystem services in China's Loess Plateau: Patterns, interactions, drivers, and implications. Glob Planet Change. 160, 41-52. https://doi.org/10.1016/j.gloplacha.2017.11.014.

Kienast, F., Frick, J., van Strien, M.J., Hunziker, M., 2015. The Swiss Landscape Monitoring Program—a comprehensive indicator set to measure landscape change. Ecol Model. 295, 136-150. https://doi.org/10.1016/j.ecolmodel.2014.08.008.

Lee, H., Lautenbach, S., 2016. A quantitative review of relationships between ecosystem services. Ecol. Ind. 66, 340-351. https://doi.org/10.1016/j.ecolind.2016.02.004. https://doi.org/10.1016/j.ecolind.2016.02.004.

Legendre, P., Legendre, L., 2012. Numerical ecology, 3rd edition. Developments in Environmental Modelling Vol. 24 Elsevier Science BV, Amsterdam.

Li, F., Zhang, S.W., Yang, J.C., Bu, K., Wang, Q., Tang, J.M., Chang, L.P., 2016. The effects of population density changes on ecosystem services value: a case study in Western Jilin, China. Ecol Indic. 61, 328-337. https://doi.org/10.1016/j.ecolind.2015.09.033.

Li, J., 1999. Ecological value theory. Chongqing, China: Chongqing University Press.

Li, S., Liang, W., Fu, B.J., et al., 2016. Vegetation changes in recent large-scale ecological restoration projects and subsequent impact on water resources in China's Loess Plateau. Sci Total Environ. 569-570, 1032-1039. https://doi.org/10.1016/j.scitotenv.2016.06.141.

Li, Y.R., Cao, Z., Long, H.L., et al., 2017. Dynamic analysis of ecological environment combined with land cover and NDVI ch-anges and implications for sustainable urban-rural development: The case of Mu Us Sandy Land, China. Journal of Cleaner Production. 142, 697-715. https://doi.org/10.1016/j.jclepro.2016.09.011.

Liu, B.Y., Nearing, M.A., Nearing, M.A., Risse, L.M., 2000. Slope Length Effects on Soil Loss for Steep Slopes. Soil Sci. Soc. Am. J. 64, 1759-1763. https://doi.org/10.2136/sssaj2000.6451759x.

Liu, Y., Bi, J., Lv, J.S., Ma, Z.W., Wang, C., 2017. Spatial multi-scale relationships of ecosystem services: A case study using

a geostatistical methodology. Sci Rep. 7, 9486. https://doi.org/10.1038/s41598-017-09863-1.

Lufafa, A., Tenywa, M.M., Isabiarye, M., Majaliwa, M.J.B., Woomer, P.L., 2003. Predication of soil erosion of in a Lake Victoria basin catchment using GIS-based Universal Soil Loss model. Agr. Syst. 76, 883-894. https://doi.org/10.1016/S0308-521X(02)00012-4.

Lü, Y.H., Fu, B.J., Feng, X.M, Zeng, Y., Liu, Y., Chang, R.Y., Sun, G., Wu, B.F., 2012. A policy driven large scale ecological restoration: quantifying ecosystem services changes in the Loess Plateau of China. PLoS One. 7, 31782. https://doi.org/10.1371/journal.pone.0031782.

Lyu, R., Clarke, Keith., Zhang, J.M., Feng, J.L., Jia, X.H., Li, J.J., 2019. Spatial correlations among ecosystem services and their socio-ecological driving factors_ A case study in the city belt along the Yellow River in Ningxia, China. Appl. Geogr. 108, 64-73. https://doi.org/10.1016/j.apgeog.2019.05.003.

MA (Millennium Ecosystem Assessment), 2005. Overview of the Millennium Ecosystem Assessment. Available from http://www.millenniumassessment.org/en/About.html#, . accessed July 2017.

Ma, T.T., Li, X.W., Bai, J.H., Ding, S.Y., Zhou, F.W., Cui, B.S., 2019. Four decades' dynamics of coastal blue carbon storage driven by land use/land cover transformation under natural and anthropogenic processes in the Yellow River Delta, China. Sci Total Environ. 655, 741-750. https://doi.org/10.1016/j.scitotenv.2018.11.287.

Ma, Z.Z., 1989. A method for determining factors of USLE by using satellite photos. Soil Water Conserv CHN. 3, 24-27.

Meacham, M., Queiroz, C., Norström, A.V., Peterson, G.D., 2016. Social-ecological driver of multiple ecosystem services: what variables explain patterns of ecosystem services across the Norrström drainage basin? Ecol. Soc. 21, 14. http://dx.doi.org/10.5751/ES-08077-210114.

Mccool, D.K., Foster, G.R., Mutchler, C.K., Meyer, L.D., 1989. Revised Slope Length Factor for the Universal Soil Loss Equation. Trans. ASAE. 32, 1571-1576. https://doi.org/10.13031/2013.30576.

Mouchet, M.A., Lamarque, P., Martin-Lopez, B., Crouzat, E., Gos, P., Byczek, C., Lavorel, S., 2014. An interdisciplinary methodological guide for quantifying associations between ecosystem services. Global Environ. Change 28, 298-308. http://dx.doi.org/10.1016/j.gloenvcha.2014.07.012.

Mouchet, M.A., Paracchini, M.L., Schulp, C.J.E., Stürck, J., Verkerk, P.J., Verburg, P.H., Lavorel, S., 2017. Bundles of ecosystem(dis)services and multifunctionality across European landscapes. Ecol. Indic. 73, 23-28. https://doi.org/10.1016/j.ecolind.2016.09.026.

Ndong, G.O., Therond, O., Cousin, I., 2020. Analysis of relationships between ecosystem services: A generic classification and review of the literature. Ecosyst Serv. 43, 101-120. https://doi.org/10.1016/j.ecoser.2020.101120.

Peng, J., Chen, X., Liu, Y.X., Lu, H.L., Hu, X.X., 2016. Spatial identification of multifunctional landscapes and associated influencing factors in the Beijing-Tianjin-Hebei region, China. Appl. Geogr. 74, 170-181. https://doi.org/10.1016/j.apgeog.2016.07.007.

Peng, J., Tian, L., Liu, Y.X., Zhao, M.Y., Hu, Y.N., Wu, J.S., 2017. Ecosystem services response to urbanization in metropolitan areas: Thresholds identification. Sci Total Environ. 607-608, 706-714. http://dx.doi.org/10.1016/j.scitotenv.2017.06.218.

Potter, C.S., Randerson, J.T., Field, C.B., Matson, P.A., Mooney, H.A., Klooster, S.A., 1993. Terrestrial ecosystem production: A process model based on global satellite and surface data. Global Biogeochem Cycles. 7, 811-841. https://doi.org/10.1029/93GB02725.

Qiu, J.X, Turner, M.G., 2013. Spatial interactions among ecosystem services in an urbanizing agricultural watershed. Proc. Natl. Acad. Sci. U. S. A. 2013, 12149-12154. https://doi.org/10.1073/pnas.1310539110.

Queiroz, C., Meacham, M., Richter, K., Norström, A.V., Andersson, E., Norberg, J., Peterson, G., 2015. Mapping bundles of ecosystem services reveals distinct types of multifunctionality within a Swedish landscape. Ambio. 44, 89-101. https://doi.org/10.1007/s13280-014-0601-0.

Quintas-Soriano, C., García-Llorente, M., Norström, A., Meacham, M., Peterson, G., Castro, A.J., 2019. Integrating supply and demand in ecosystem service bundles characterization across Mediterranean transformed landscapes. Landscape Ecol. 34, 1619-1633. https://doi.org/10.1007/s10980-019-00826-7.

Raudsepp-Hearne, C., Peterson, G.D., Bennett, E.M., Mooney, H.A., Naturvetenskapliga, F., Stockholm, R.C., Institutionen, F.N.O.K., Stockholms, U., 2010. Ecosystem service bundles for analyzing tradeoffs in diverse landscapes. P. Natl. Acad. Sci. Usa. 107, 5242-7. https://doi.org/10.1073/pnas.0907284107.

Raudsepp-Hearne, C., Peterson, G.D., 2016. Scale and ecosystem services: How do observation, management, and analysis shift with scale-lessons from Québec. Ecol. Soc. 21: 16. https://dx.doi.10.5751/ES-08605-210316.

Renard, K.G., Foster, G.R., Weesies, G.A., Porter, J.P., 1991. RUSLE: revised universal soil loss equation. J. Soil Water Conserv. 46(1), 30-33.

Renard, D., Rhemtulla, J.M., Bennett, E.M., 2015. Historical dynamics in ecosystem service bundles. Proc. Natl. Acad. Sci.

U.S.A. 112 (43), 13411-13416. https://doi.org/cgi/doi/10.1073/pnas.1502565112.

Rodríguez, J.P., Beard, T.D., Bennett, E.M., Cumming, G.S., Cork, S.J., Agard, J., Dobson, A.P., Peterson, G.D., 2006. Trade-offs across Space, Time, and Ecosystem Services. Ecol. Soc. 11, 28. https://doi.org/10.5751/ES-01667-110128.

Rositano, F., Bert, F.E., Piñeiro, G., Ferraro, D.O., 2018. Identifying the factors that determine ecosystem services provision in Pampean agroecosystems (Argentina) using a data-mining approach. Enviro Dev. 25, 3-11, https://doi.org/10.1016/j.envdev.2017.11.003.

Schirpke, U., Candiago, S., Vigl, L.E., Ja¨ger, H., Labadini, A., Marsoner, T., Tappeiner, U., 2019. Integrating supply flow and demand to enhance the understanding of interactions among multiple ecosystem services. Sci Total Environ. 651, 928-941. https://doi.org/10.1016/j.scitotenv.2018.09.235.

Schulze, J., Frank, K., Priess, J.A., Meyer, M.A., 2016. Assessing regional-scale impacts of short rotation coppices on ecosystem services by modeling land-Use decisions. PLoS One. 11, 0153862. https://doi.org/10.1371/journal.pone.0153862.

Spake, R., Lasseur, R., Crouzat, E., Bullock, J.M., Lavorel, S., Parks, K.E., Schaafsma, M., Bennett, E.M., Maes, J., Mulligan, M., Mouchet, M., Peterson, G.D., Schulp, C.J.E., Thuiller, W., Turner, M.G., Verburg, P.H., Eigenbrod, F., 2017. Unpacking ecosystem service bundles: Towards predictive mapping of synergies and trade-offs between ecosystem services. Global Environ. Change. 47, 37-50. https://doi.org/10.1016/j.gloenvcha.2017.08.004.

Su, C.H., Fu, B.J., He, C.S., Lü, Y.H., 2012. Variation of ecosystem services and human activities: A case study in the Yanhe Watershed of China. Acta Oecologica. 44, 46-57. https://doi.org/10.1016/j.actao.2011.11.006.

Su, C.H., Fu, B.J., 2013. Evolution of ecosystem services in the Chinese Loess Plateau under climatic and land use changes. Glob. Planet. Chang. 101, 119-128. https://doi.org/10.1016/j.gloplacha.2012.12.014.

Tomscha, S., Gergel, S., 2016. Ecosystem service trade-offs and synergies misunderstood without landscape history. Ecol. Soc. 21, 43. https://doi.org/10.5751/ES-08345-210143.

Treacy, P., Jagger, P., Song, C., Zhang, Q., Bilsborrow, R.E., 2018. Impacts of China's Grain for Green Program on Migration and Household Income. Environ. Manage. 62, 489-99. https://doi.org/10.1007/S00267-018-1047-0.

Turner, K.G., Odgaard, M.V., Bøcher, P.K., Dalgaard, T., Svenning, J., 2014. Bundling ecosystem services in Denmark: Trade-offs and synergies in a cultural landscape. Landscape Urban Plan. 125, 89-104. https://doi.org/10.1016/j.landurbplan.2014.02.007.

Wang, C.D., Li, X., Yu, H.J., Wang, Y.T., 2019. Tracing the spatial variation and value change of ecosystem services in Yellow River Delta, China. Ecol. Indic. 96, 270-7. https://doi.org/10.1016/j.ecolind.2018.09.015.

Wang, J.F., Li, X.H., Christakos, G., Liao, Y.L., Zhang, T., Gu, X., Zheng, X.Y., 2010. Geographical Detectors-based health risk assessment and its application in the Neural Tube Defects study of the Heshun Region, China. Int. J. Geogr. Inf. Sci. 24, 107-127. https://doi.org/10.1080/13658810802443457.

Wang, J.F., Zhang, T.L., Fu, B.J., 2016. A measure of spatial stratified heterogeneity. Ecol. Indic. 67, 250-256. https://doi.org/10.1016/j.ecolind.2016.02.052.

Wang, X.F., Xiao, F.Y., Feng, X.M., Fu, B.J., Zhou, Z.X., Chan, C., 2019. Soil conse[illegible]ation on the Loess Plateau and the regional effect: impact of the 'Grain for Green' Project. Earth Environ S[illegible] Tra[illegible]s R Soc Edinb. 109, 461-471. https://doi.org/10.1017/S1755691018000634.

Wischmeier W.H., Smith D.D. 1978. Predicting Rainfall Erosion Losses –A G[illegible]ide to conservation planning.

Williams, J.R., 1990. The erosion-productivity impact calculator (F[illegible]) model: a case history Philos. Trans. R. Soc. Lond. 329, 421-428. http://dx.doi.org/10.1098/rstb.1990.0184.

Wong, C.P., Jiang, B., Kinzig, A.P., Lee, K.N., Ouyang, Z.Y., 2015. Linking ecosystem characteristics to final ecosystem services for public policy. Ecol. Lett. 18 (1), 108-1[illegible]

Xi, J.P. Speech at the symposium o[illegible]ological protection and high-quality development in the Yellow River Basinhthttps://www.xinhuanet.com/[illegible]19-10/15/c_1125107042.htm. (accessed 15 October 2019).

Yang, G.F., Ge, Y., Xue, H., Yang, W., Shi, Y., Peng, C.H., Du, Y.Y., Fan, X., Ren, Y., Chang, J., 2015 Using ecosystem service bundles to detect trade-offs and synergies across urban-rural complexes. Landsc. Urban Plan. 136, 110-121. https://doi.org/10.1016/j.landurbplan.2014.12.006.

Zhang, Y.Y., Zhang, S.F., Zhai, X.Y., Xia, J., 2012. Runoff variation and its response to climate change in the Three Rivers Source Region. J. Geogra. Sci. 22, 781-794. https://doi.org/10.1007/s11442-012-0963-9.

Zhao, T.Q., Ouyang, Z.Y., Zheng, H., Wang, X., Hong, M., 2004. Forest ecosystem services and their valuation in China. J. Nat. Resour. 19, 480-491. https://doi.org/10.1007/BF02873086.

Zhou, Z.X., Li, J., Guo, Z.Z., Li, T., 2017. Trade-offs between carbon, water, soil and food in Guanzhong-Tianshui economic region from remotely sensed data. Int J Appl Earth Obs Geoinf. 58, 145-156. https://doi.org/10.1016/j.jag.2017.01.003.

Zhu, W.Q., Pan, Y.Z., Yang, X.Q., et al., 2007. Comprehensive analysis of the impact of climatic changes on Chinese

terrestrial net primary productivity. Chinese Sci Bull. 52, 3252-3260. https://doi.org/10.1007/s11434-007-0521-5.

Credit Author Statement

Y Zhang and X Lu designed the study, collected the database and performed the research. Y Zhang analyzed data, and wrote the paper. B Liu participated in data processing and model calculation. The remaining authors contributed to discuss the results and revise the manuscript. All authors have read and approved this manuscript.

Declaration of Interest Statement

The authors declare that there is no conflict of interest regarding the publication of this article.

Graphical abstract

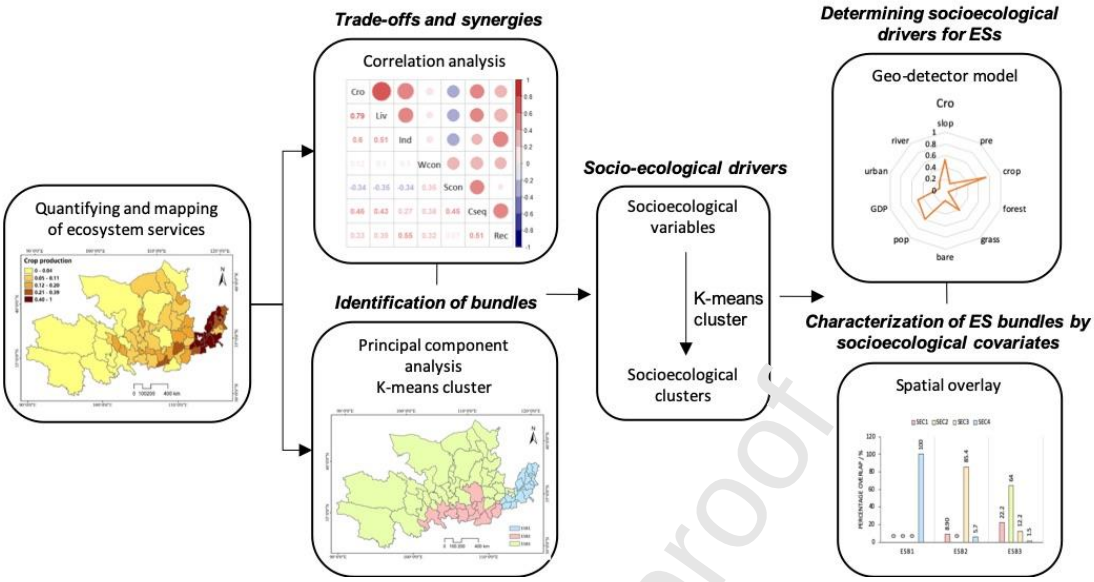

Highlights:

- The synergies between ESs substantially exceeded the trade-offs.
- Trade-offs occurred between provisioning services and soil conservation.
- Three bundles were identified, distinct differentiation in the groupings of ESs.
- Land use/land cover strongly affected the characteristics of the ES bundles.